

Bimetallic Cu/Fe Catalysts for Ibuprofen Mineralization

Sajid Hussain, Eleonora Aneggi *, Daniele Goi and Alessandro Trovarelli

Dipartimento Politecnico di Ingegneria e Architettura, Università di Udine, Unità di Ricerca INSTM Udine, 33100 Udine, Italy; hussain.sajid@spes.uniud.it (S.H.); daniele.goi@uniud.it (D.G.); alessandro.trovarelli@uniud.it (A.T.)

* Correspondence: eleonora.aneggi@uniud.it; Tel.: +39-0432-558847

Abstract: At present, the use of conventional wastewater processes is becoming increasingly challenging, mainly due to the presence of biorecalcitrant organic matter. Advanced oxidation processes such as Fenton, Fenton-like and hybrid processes have been successfully employed for the treatment of highly concentrated and toxic non-biodegradable pollutants. Here, a series of bimetallic catalysts, based on Cu/Fe supported over ZrO₂, were investigated for the mineralization of ibuprofen with a heterogeneous Fenton-like reaction. The materials were prepared by incipient wetness impregnation and characterized by standard techniques. Temperature-programmed experiments highlighted the promotion of the reduction in CuO due to the synergistic effects of the coupled redox cycles of copper (Cu²⁺/Cu⁺) and iron (Fe⁺³/Fe⁺²). 5%Cu-5%Fe/ZrO₂ not only displays the highest ibuprofen mineralization (83%) under optimum conditions but also exploits its activity in a wider range of pH (3–5) with extremely low metal leaching. The recycling of bimetallic catalysts reveals that only the 5%Cu-5%Fe/ZrO₂ system is able to provide sustainable activity in heterogeneous Fenton process.

Keywords: Fenton-like oxidation; heterogeneous reaction; bimetallic catalyst; ibuprofen; wastewater treatment

Citation: Hussain, S.; Aneggi, E.; Goi, D.; Trovarelli, A. Bimetallic Cu/Fe Catalysts for Ibuprofen Mineralization. *Catalysts* **2021**, *11*, 1383. <https://doi.org/10.3390/catal11111383>

Academic Editor: Gilles Berhault

Received: 27 October 2021

Accepted: 14 November 2021

Published: 16 November 2021

Publisher's Note: MDPI stays neutral with regard to jurisdictional claims in published maps and institutional affiliations.



Copyright: © 2021 by the authors. Licensee MDPI, Basel, Switzerland. This article is an open access article distributed under the terms and conditions of the Creative Commons Attribution (CC BY) license (<http://creativecommons.org/licenses/by/4.0/>).

1. Introduction

Water contamination has become a very serious challenge due to the release of large numbers of refractory pollutants into water bodies [1–3]. Global environmental protection agencies have progressively enforced very stringent guidelines to safeguard ground and surface waters [4]; however, the conventional biological processes cannot efficiently eliminate the persistent organic pollutants, and robust abatement technologies must be used [5]. Among the advanced oxidation processes (AOPs), the Fenton process is very effective for the abatement of refractory organics due the utilization of highly reactive and non-selective hydroxyl radicals ($\cdot\text{OH}$) [6,7]. Although the homogeneous Fenton process is very simple, efficient and cost-effective, it produces large volumes of residual sludge, which needs to be processed and disposed of, creating another environmental challenge [8,9]. Moreover, the process is only efficient under acidic pH conditions, i.e., pH 3 and this induces additional chemical costs [10,11]. These drawbacks can be overcome by employing the heterogeneous Fenton process as this does not produce sludge and the catalyst is easily separated from the liquid stream and can be reused [12–14]. However, iron-based heterogeneous materials still require acidic conditions to achieve high process efficiencies and catalysts become more susceptible to higher amounts of metal leaching [15,16]. Furthermore, the iron-based formulations have a tendency to form complexes with the degradation products, with the consequent deactivation of the catalyst [17,18].

Improving the efficiency and stability of the process is possible through the coupling of Fenton reaction with different technologies, such as ultrasound (US), ozone (O₃) or ultraviolet radiation (UV) [19–25]. Generally, among the hybrid processes, homogeneous or heterogeneous Fenton coupled with UV reaches high degrees of mineralization [20,26]. Another method of increasing the performance of the Fenton processes is to develop more

active formulations; the catalytic activity of materials based on transition metals, such as copper, silver, manganese [16,27–34], supported over different metal oxide, has been widely investigated, obtaining fairly good catalytic performance. However, each material achieves a higher mineralization under different optimal reaction conditions, such as pH, catalyst loading and oxidant dose and, consequently, the overall experimental setup should be considered in the comparison between catalytic activities [16,30,31]. Due to the narrow working optimal pH offered by monometallic catalysts during the Fenton reaction, the optimization of the process is itself a great challenge as the slightest variation in the pH of the aqueous solution may significantly reduce the overall efficacy. Bimetallic catalysts employing two transition metals over an appropriate support may eliminate all these limitations and further enhance the efficiency of the heterogeneous Fenton process [35].

In a previous study, we developed very active materials based on copper or iron oxides supported over zirconia for the treatment of ibuprofen (IBP) in a Fenton-like reaction [16]. Although Cu/ZrO₂ and Fe/ZrO₂ afforded very high catalytic activities, some limitations, such as the narrow working pH, metallic leaching and complexation, inspired us to attempt the development of new and more active heterogeneous catalysts based on bimetallic iron and copper composite materials. The effects of total metal loading and iron/copper ratio on catalytic activity were investigated under varying pH, catalyst loading, H₂O₂ dose and temperature conditions, with the traditional “one-factor-at-a-time” method [36]. In addition, the catalytic performances of all these catalysts were observed after recycling. Overall, bimetallic formulations were found to be more active and more stable compared to monometallic catalysts. The synergistic effect of the coupled redox cycles of copper and iron significantly boosted the mineralization of ibuprofen, and removed some limitations observed in single component counterparts. This resulted in novel and more attractive catalysts for Fenton-like reactions.

2. Results

2.1. Catalyst Characterization

The composition and BET surface area of the materials are reported in Table 1. The addition of Cu and Fe does not strongly affect the surface area of pure zirconia (64 m²/g), with a maximum decrease to 55 m²/g occurring independently over the total loading of transition metals. Similarly, crystallite size varies in the range 12–13 nm.

Table 1. Composition and surface area of investigated samples.

Sample	Composition	Crystallite Size ^a (nm)	Surface Area (m ² /g)
2.5Cu/2.5Fe	Cu(2.5 wt.%)–Fe(2.5 wt.%)//ZrO ₂	13	59
2.5Cu/5Fe	Cu(2.5 wt.%)–Fe(5 wt.%)//ZrO ₂	12	55
5Cu/2.5Fe	Cu(5 wt.%)–Fe(2.5 wt.%)//ZrO ₂	13	59
5Cu/5Fe	Cu(5 wt.%)–Fe(5 wt.%)//ZrO ₂	12	55

^a: calculated with Scherrer formula from X-ray diffraction patterns.

The structural features of the zirconia-based materials were analyzed by powder X-ray diffraction (XRD).

Zirconia support is composed of monoclinic (space group P121/c1) and tetragonal ZrO₂ (space group P42/nmc), as shown in Figure 1. There is no evidence for any other reflection, suggesting a homogeneous dispersion of copper and iron phase on the surface. Main signals of Fe₂O₃ and CuO are overlapped by reflections of zirconia; consequently, a detailed analysis of XRD profiles is needed to obtain insight into iron and copper phases. Table 2 shows the assignment of some important signals to the various oxides.

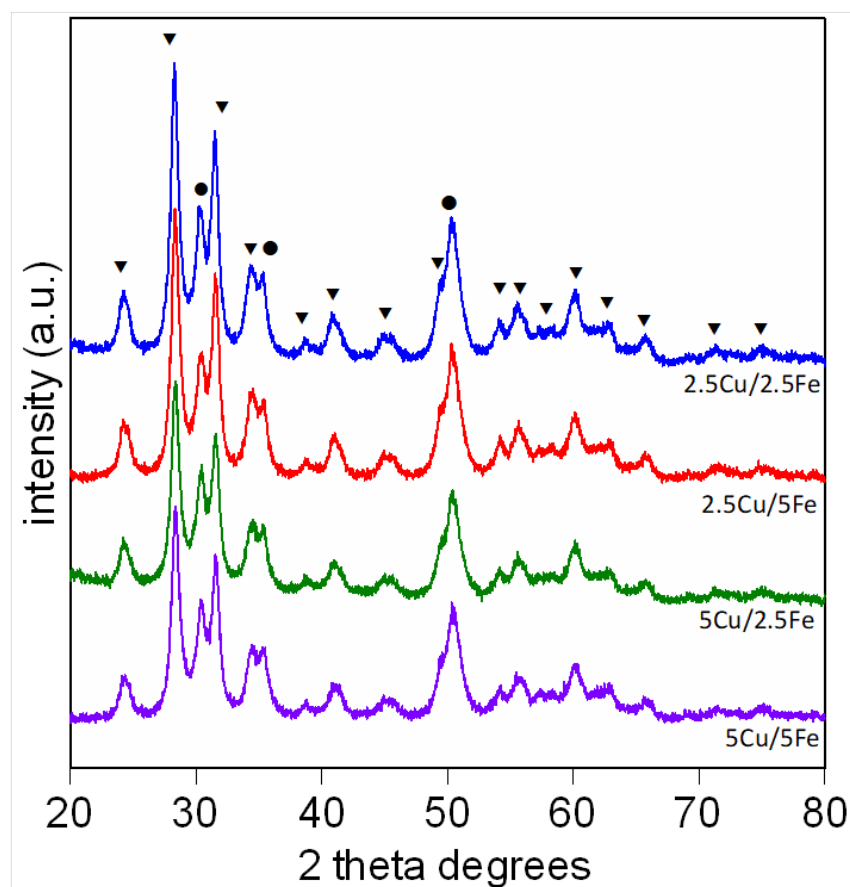


Figure 1. XRD profiles of the investigated bimetallic formulations (▼ monoclinic ZrO₂, ● tetragonal ZrO₂)

Table 2. Assignment of signals in XRD profile.

2θ (°)	Phase
24.3	ZrO ₂ ; Fe ₂ O ₃
28.2	ZrO ₂
34.2	ZrO ₂
35.6	ZrO ₂ ; CuO; Fe ₂ O ₃
54.1	ZrO ₂ ; Fe ₂ O ₃

Reflection at 28.2° and 34.2° is assigned to ZrO₂, while signals at 24.3° and 54.1° are due to ZrO₂ and Fe₂O₃. Under the reflection at 35.6°, signals are found due to ZrO₂, Fe₂O₃ and CuO. The relative intensity of specific signals at the variation in metal loadings gives some information on the presence of iron and copper oxides (Figure 2). Specifically, Fe₂O₃ can be recognized by the increased relative intensity of reflections at 24.3° and 54.1° with respect to signal at 28.2°, attributable to monoclinic ZrO₂, as the amount of iron added to the support increases. For CuO the ratio between signals at 35.6° and 34.2° is used. The progressive increase in this intensity ratio, with the Cu loading, indicates the presence of CuO.

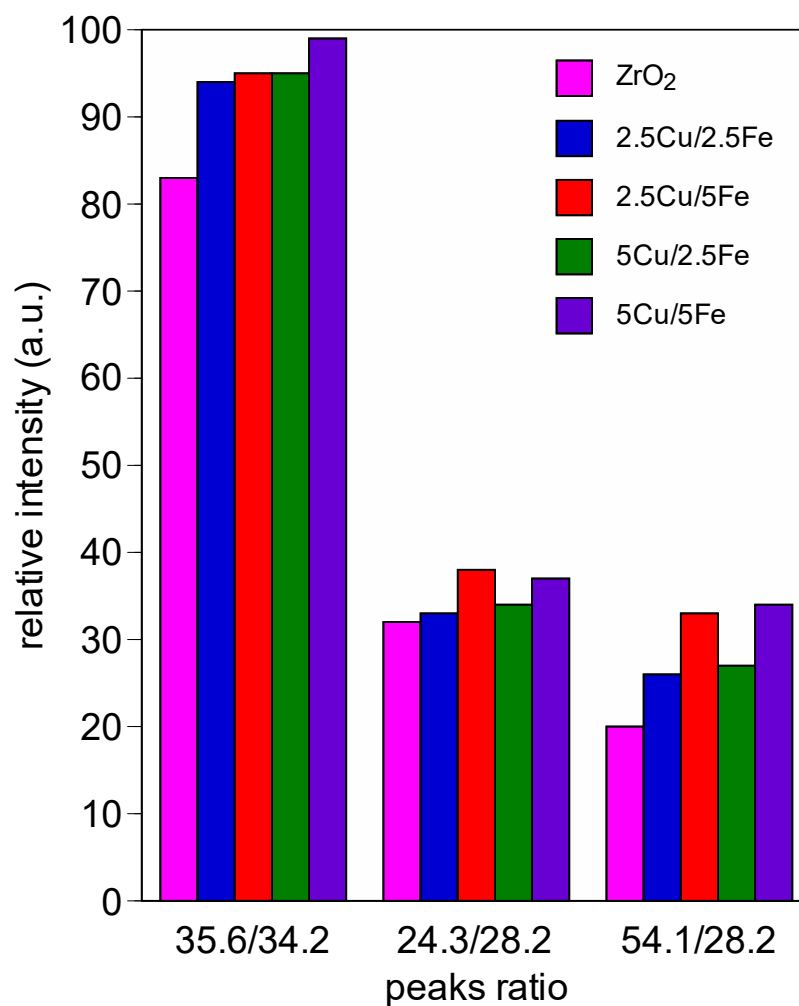


Figure 2. Relative intensity of main characteristic signals of ZrO₂, Fe₂O₃ and CuO.

The reduction behavior of the bimetallic catalysts has been investigated by means of H₂ temperature-programmed reduction experiments (H₂-TPR) (Figure 3). All the materials exhibit four peaks due to the reduction in CuO and Fe₂O₃ [37]. Specifically, the reduction profile is characterized by three peaks in the temperature range 120–300 °C: the first one (α peak), in the range 140–150 °C is attributed to the reduction in highly dispersed CuO, while the signal in the range 230–265 °C (γ peak), is due to the reduction in bulk CuO [38]. The second signal at 200–220 °C (β peak) corresponds with the reduction of Fe₂O₃ to Fe₃O₄. Finally, at 300–400 °C a broad signal (δ peak) is found due to the further reduction of Fe₃O₄ to Fe [39]. Samples with 5% of Fe show a more intense β peak and a broad δ peak compared to formulations with 2.5%, as expected, with no substantial changes in signal temperature. A more significant difference can be found for γ signals related to CuO reduction. Indeed, when the iron amount is 2.5 wt.%, the signals are in the range 255–265 °C, while the peak is shifted to a lower temperature (230–240 °C) for samples with 5 wt.% of iron (2.5Cu/5Fe and 5Cu/5Fe). The promotion of the reduction in CuO can be due to the synergistic effects between Fe₂O₃ and CuO. This effect, related to the coupled redox cycles of copper (Cu²⁺/Cu⁺) and iron (Fe³⁺/Fe²⁺), improves the reducibility of the materials and is more pronounced with the 5Cu/5Fe formulation, which shows higher reducibility at a low temperature.

Summarizing, the characterization of the developed materials indicates that the bimetallic catalysts show a very similar surface area and crystallite size and, consequently, these parameters do not significantly affect the catalytic activity. The active phases on the zirconia surface are metal oxides of copper and iron and, specifically, CuO (Cu²⁺) and

Fe_2O_3 (Fe^{3+}), as clearly evidenced by XRD analysis. In addition, a homogeneous dispersion of copper and iron phase on the surface has been highlighted.

The four bimetallic catalysts show the main differences in the reduction behavior, with an important promotion of the reducibility at low temperatures for 5Cu/5Fe material. This promotion is related to the synergistic effects of the two metal oxides and is more pronounced for the highest amount of metals and for an equal mole ratio of copper and iron.

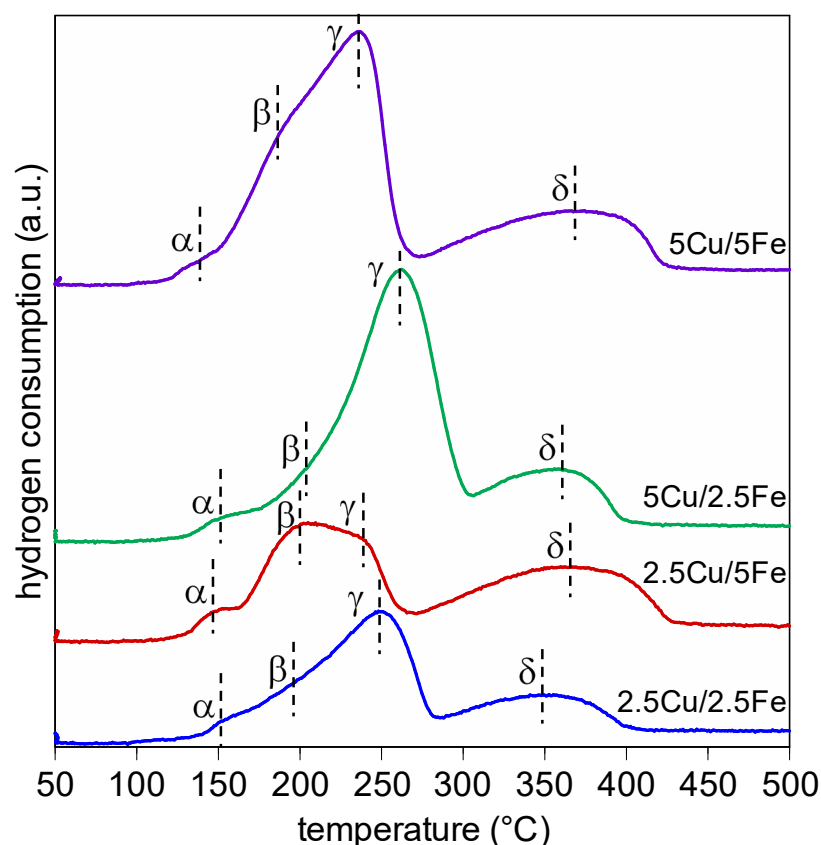


Figure 3. H_2 -TPR profiles of the investigated samples.

2.2. Catalytic Activity

The pH of the aqueous solution is the most critical parameter in heterogeneous Fenton process as the catalyst can only produce a maximum amount of $\cdot\text{OH}$ from the oxidant within a specific range of pH conditions, achieving increased catalytic activity [36]. To investigate the activities of bimetallic catalysts, the oxidation reactions were performed over a broader pH range and the results are presented in Figure 4. For all the materials the highest IBP mineralization (i.e., conversion to CO_2 and H_2O) was achieved in the first 30 min and, for longer times, the catalytic activity does not show significant variation. This indicates that the mineralization of the parent molecule is a very fast process. Complete mineralization cannot be achieved due to the conversion of IBP into secondary compounds that cannot be easily degraded.

All bimetallic catalysts have shown very high and stable mineralization of IBP (~70–80%) within the pH range of 3–4 and, unlike monometallic catalysts, these formulations have a wider window of optimal pH, through which they can achieve maximum total organic carbon (TOC) removal [5,40]. The activity of bimetallic materials can be related to the synergistic effect of the coupled redox cycles of copper ($\text{Cu}^{2+}/\text{Cu}^+$) and iron $\text{Fe}^{3+}/\text{Fe}^{2+}$

(Figure S1) [41]. However, when the Fenton process is conducted at pH 5, the TOC abatement dropped to 50–55% for 2.5Cu/2.5Fe, 2.5Cu/5Fe and 5Cu/2.5Fe, suggesting that pH plays an important role in the efficacy of these bimetallic formulations in the Fenton process.

A different situation arises for 5Cu/5Fe, which displayed the highest activity at pH 4 (83%), immediately followed by pH 3 (80%). At pH 5, 5Cu/5Fe is definitely more active, with mineralization of 65%, compared to the other formulations (50–55%). 5Cu/5Fe shows the highest activity in the range of pH 3–4, but also maintains high TOC abatement at pH 5, indicating a broad operating pH. This effect is probably due to the promotion of the reducibility caused by the synergistic effect of copper and iron redox cycles, as found in H₂-TPR experiments.

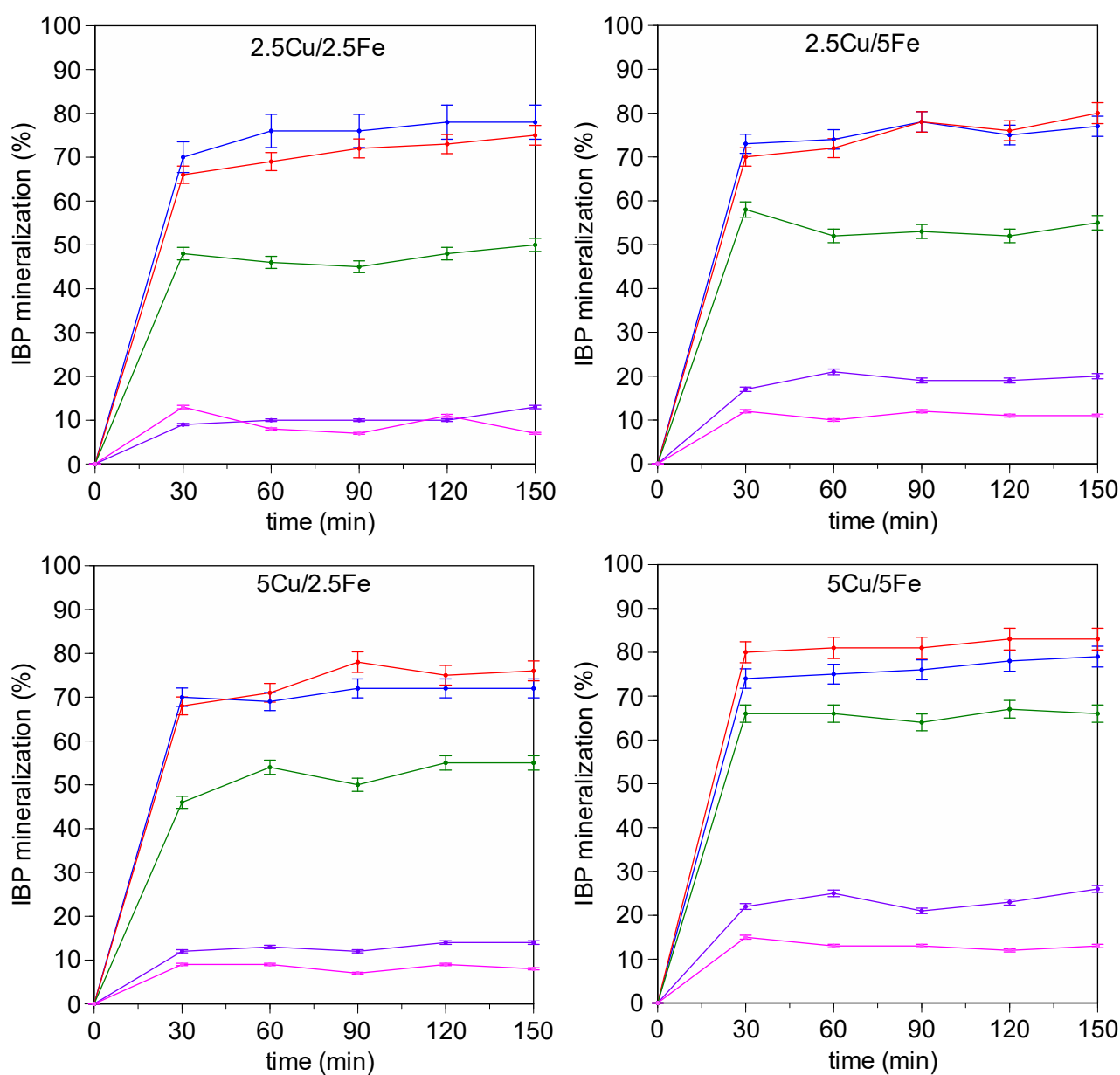


Figure 4. Effect of pH on the IBP mineralization by bimetallic catalysts: pH 3 blue, pH 4 red, pH 5 green, pH 6 purple, pH 8 pink. (Reaction condition: catalyst dose—200 mg/L, H₂O₂ dose—30 mL/L, temperature —70 °C).

The IBP mineralization is dramatically reduced to 10–20% when the operating pH is increased to 6 and 8. These results indicate that, under near-neutral to basic conditions,

the oxidant starts decomposing into oxygen and water and the efficiency is suppressed [42]. In sum, pH 4 achieved maximum TOC abatements with a relatively less acidic condition compared to pH 3 and this is advantageous as chemical costs are reduced, while metal leaching is minimized. Therefore, the optimization of the other variables was performed at pH 4. Notably, the ratios of iron and copper in the bimetallic samples also govern the extent to which these catalysts can exercise a bimetallic redox cycle. For instance, the 2.5Cu/5Fe and 5Cu/2.5Fe catalysts can only exhibit the characteristics of bimetallic catalysts through 50% of its sites as the total fraction of the limiting metal component is 0.5, while the rest of the material will exhibit the characteristics of monometallic catalysts (Figure S2). Conversely, 2.5Cu/2.5Fe and 5Cu/5Fe can express the features of full bimetallic catalysts as both metals are charged onto the support in equal mole ratios. These adjustments in the ratios of the two metallic parts not only aid in building robust and highly active materials, but also reduce the overall cost of the catalyst. The stabilities of all these bimetallic catalysts were examined at pH 3 and 4 as they experienced maximum activity under these conditions, and the results are presented in Figure 5.

The results clearly suggest that iron leaching from the bimetallic catalysts is substantially lower than copper and changes with varying pHs are negligible, indicating stronger bonds of iron atoms with the support material. On the other hand, copper leaching is significant at pH 3, as reported in a previous study [16]; however, this is reduced at pH 4, suggesting that the stability of copper atoms is strongly affected under acidic conditions. Specifically, iron leaching is always lower than 5%, while copper leaching at pH 4 is between 5 and 10%. Notably, none of the catalysts at pH 4 exceeded the maximum limits set by the European Union for the amount of iron and copper in treated water [41,43,44].

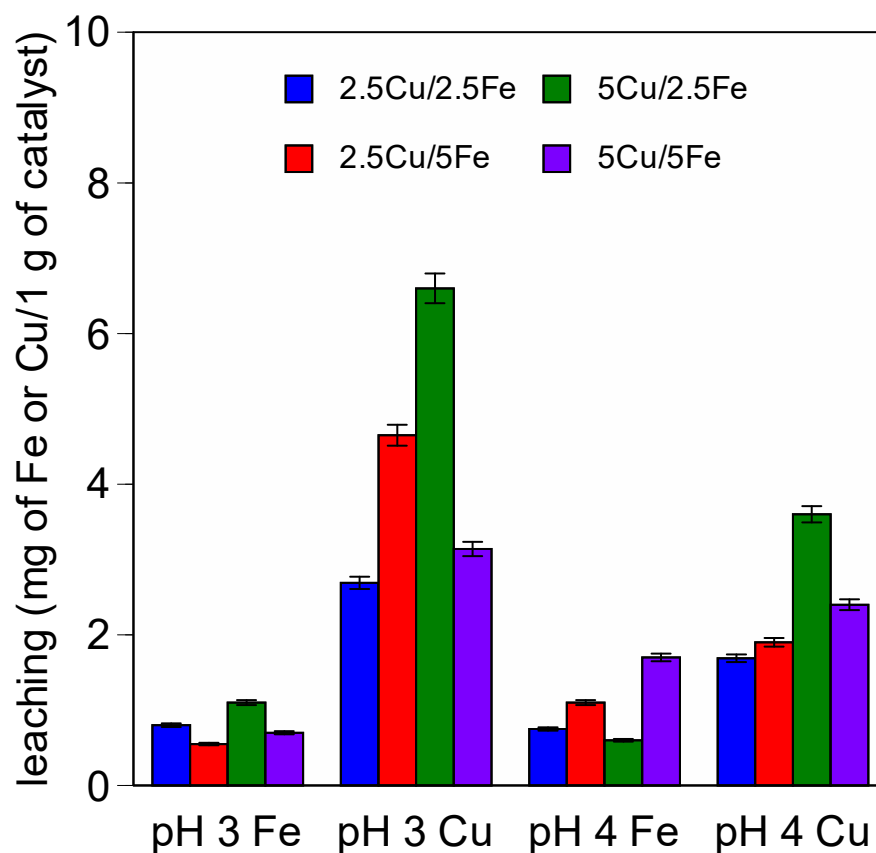


Figure 5. Iron and copper leaching at pH 3 and 4 (reaction conditions: catalyst dose—200 mg/L, H₂O₂ dose—30 mL/L, temperature—70 °C).

Generally, increasing the catalyst dose increases the efficacy of the Fenton process, y the optimum catalyst amount ought to be experimentally determined to maintain the economic feasibility of the process [45]. Variable catalyst loading was used to evaluate the influence of this parameter on the overall efficacy of the oxidation process, and the results are shown in Figure 6A. The IBP mineralization over 2.5Cu/2.5Fe, 2.5Cu/5Fe and 5Cu/2.5Fe is not significantly affected by catalyst dose. These results clearly indicate that the optimal catalyst loading to achieve the best catalytic activity is 200 mg/L [41]. However, for 5Cu/5Fe, a progressive increase in the catalyst dose induces a decrease in TOC removal (from 83% to 55%), suggesting that a higher catalyst loading produces a very strong scavenging effect, with a drastic reduction of the performance of the material [46,47].

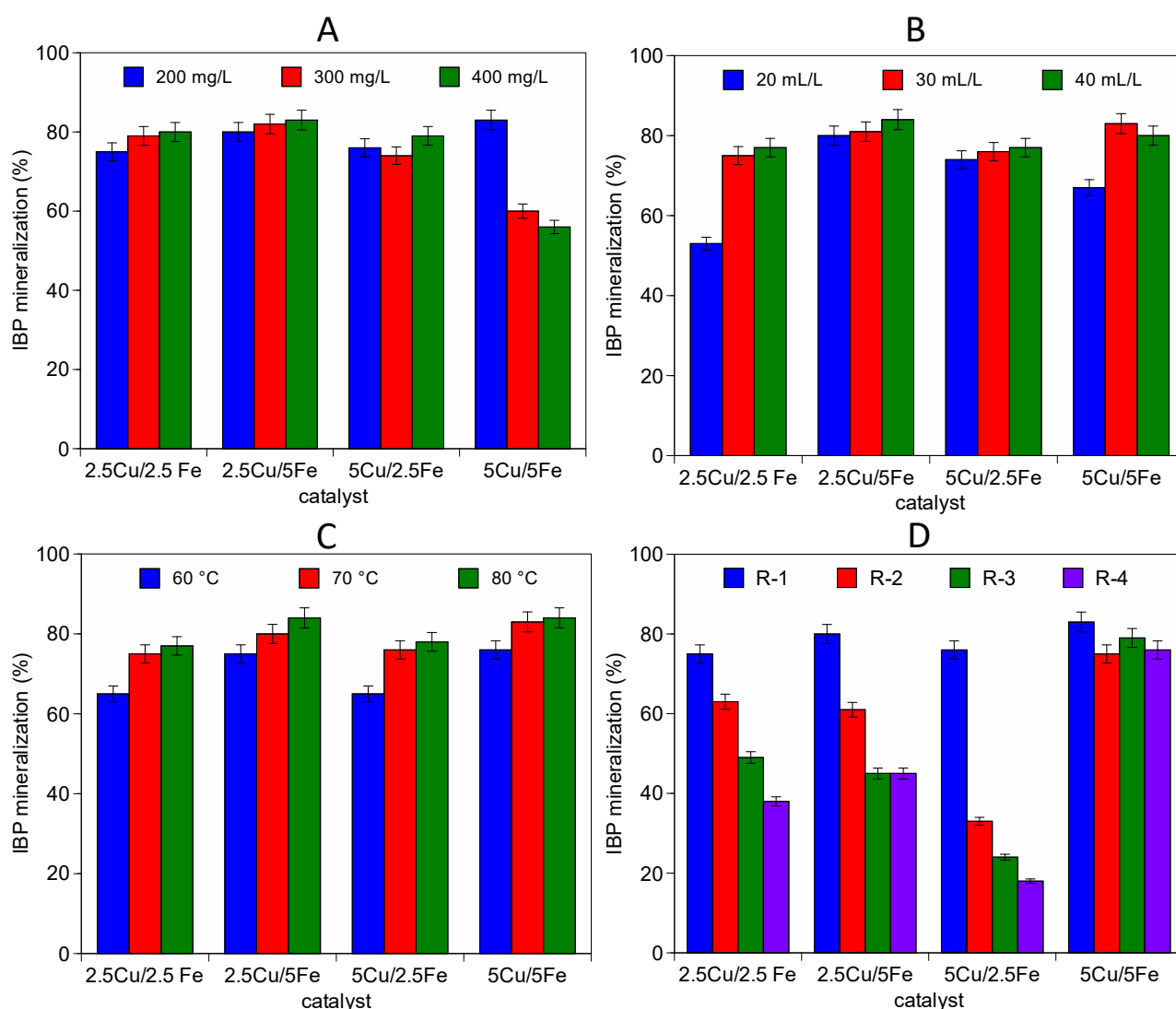


Figure 6. Effect on catalytic activity for (A) catalyst dose; (B) H₂O₂ dose; (C) temperature; (D) catalyst recycling. (reaction condition: pH 4, reaction time 150 min; (A) H₂O₂ dose—30 mL/L, 70 °C; (B) catalyst dose—200 mg/L, 70 °C; (C) catalyst dose—200 mg/L, H₂O₂ dose—30 mL/L; (D) catalyst dose—200 mg/L, H₂O₂ dose—30 mL/L, 70 °C).

In heterogeneous Fenton processes, H₂O₂ is the source of •OH free radicals and controlling the oxidant dose may help to optimize the process efficacy. The IBP mineralization efficacy as a function of H₂O₂ dose is shown in Figure 6B. When 20 mL/L H₂O₂ is used in

the oxidation process, 2.5Cu/2.5Fe only mineralized 53% of IBP. However, when the oxidant doses are increased to 30 and 40 mL/L, the TOC abatement sharply increased to 75 and 77%, respectively. Similarly, 5Cu/5Fe achieved 67% of IBP mineralization when 20 mL/L of H₂O₂ is used, while 30 mL/L of the oxidant increased the mineralization efficacy to 83%. However, further increasing the oxidant dose to 40 mL/L does not significantly affect the TOC abatement. On the other hand, while working with 2.5Cu/5Fe and 5Cu/2.5Fe, an almost stable IBP mineralization was obtained, despite the varying oxidant doses [45]. These outcomes suggest that a catalyst with low metal loadings (5% of total metal loading as Cu%+Fe%) would require higher oxidant doses to achieve higher TOC abatements, while formulations with sufficient metal loadings (7.5–10% of total metal loading as Cu%+Fe%) can afford optimal activities, with minimum oxidant doses, i.e., 20 mL/L, as the utilization efficacy of the oxidant is enhanced due to the bimetallic and monometallic redox cycles [48]. Moreover, excess oxidant doses may generate higher amounts of free radicals; however, the self-scavenging of •OH by the H₂O₂ (Equations (1) and (2)) may inhibit the increment in the process efficacy [49].



The influence of temperature on the performance of bimetallic catalysts as a function of TOC removal is shown in Figure 6C. The IBP mineralization increases proportionally with the rising temperature until it reaches 70 °C. Beyond this temperature the process activity does not notably rise. This also suggests that the rate of OH radical generation linearly increases with a rising temperature; however at 80 °C the oxidant also starts to thermally decompose, adversely affecting TOC abatement [45]. These results propose that 60 °C does not add sufficient thermal energy into the aqueous phase to activate the generation of large numbers of free •OH from the oxidant, thus yielding poor activity [50]. Similarly, even higher temperatures, i.e., 80 °C, seem unfavorable for both the thermal decomposition of H₂O₂ and the waste of oxidant due to side reactions [51], while 70 °C appears to be the best compromise between activity and energy saving.

The recyclable nature of the catalyst is one of the most important aspects for a heterogeneous catalyst. The bimetallic catalysts were recovered and reused (Figure 6D). 2.5Cu/2.5Fe mineralized 75% of IBP in the first cycle, but the TOC abatements gradually declined to 63, 49 and 38% in following cycles. Similar results were observed with 2.5Cu/5Fe, with a decrease in IBP mineralization from 80% to 45%. A more dramatic situation was found regarding the 5Cu/2.5Fe catalyst, which showed a dramatic reduction in degradation capacity, from 76 to 17%, when the catalyst was reused in the 4th cycle. On the contrary, the catalytic activity of 5Cu/5Fe was not significantly affected by several recycles. As such, the IBP mineralization shifted from 83% in the first cycle to 75, 78 and 76%, respectively, in the 2nd, 3rd, and 4th cycles. These results suggest that, while in the first cycle, all the bimetallic catalysts showed similar TOC abatement (70–80%), after recycling, 5Cu/5Fe appeared to be the more stable material, with an ibuprofen mineralization in the range 75–83%. These results seem to be related to a synergistic interaction between copper and iron that is more pronounced when an equal mole ratio (5Cu/5Fe) of the two metals is used. Indeed, as shown in the H₂-TPR profile, the presence of 5% of iron promotes the reducibility of CuO at lower temperature. In addition, the leaching of the metals is lower for 5Cu/5Fe, suggesting a higher stability over several cycles. This is a very important result, as finding the right composition of the two metals in the bimetallic catalyst is not only critical to achieving better catalytic activities but is equally important to maintaining their stabilities.

These outcomes show important progress in catalytic design compared to the monometallic formulations. A comparison with a previous work [16] indicates that the presence of two different metals over ZrO₂ can not only improve the catalytic activity at higher pH,

but, more importantly, can stabilize the catalyst and maintain the activity after several successive uses (Table 3).

5Cu/5Fe shows only a slightly higher mineralization than 10%Fe/ZrO₂ (83% vs. 76%, respectively), but at a higher pH (4 vs. 3) and with lower catalyst loading (200 vs. 400 mg/L). The difference with 10%Cu/ZrO₂ under the same pH and catalyst dose conditions is much bigger (83 vs. 66%). A significant difference is observed between the three catalysts after four recycles; indeed, the bimetallic catalyst maintains its very high activity (76%), while 10%Cu/ZrO₂ decreases to 60% and a dramatic loss of activity is found for 10%Fe/ZrO₂ (35%). Bimetallic catalyst are very promising materials for Fenton-like process due to the high IBP mineralization, milder reaction conditions and high stability after recycling.

In sum, characterization data evidenced the materials have very similar qualities in terms of surface area and the dispersion of active phases; however, they display important differences with regard to reducibility behavior. 5Cu/5Fe shows enhanced ibuprofen mineralization through a relatively wider pH range, eliminating the typical constraint associated with monometallic materials and, as a result, proving to be very stable. These improvements, compared to the monometallic catalysts, are mainly related to the synergistic effect of the two redox cycles of copper and iron and to the promotion of the reducibility at a low temperature. There is a strict correlation between the reducibility of the materials and its catalytic activity in IBP mineralization over the Fenton-like process.

Table 3. Comparison between monometallic and bimetallic formulation with 10% loading of transition metals.

Sample	Catalyst Dose (mg/L)	pH	IBP Mineralization (%)	IBP Mineralization 4° Cycle (%)	Ref
10Fe/ZrO ₂	400	3	76	35	[16]
10Cu/ZrO ₂	200	4	66	60	[16]
5Cu-5Fe/ZrO ₂	200	4	83	76	This study

3. Materials and Methods

3.1. Catalyst Preparation and Characterization

A series of bimetallic catalysts containing Cu and Fe (between 2.5 and 5% for each metal), supported over ZrO₂, were prepared. ZrO₂ support was prepared by calcination of zirconium hydroxides (Mel Chemicals) at 500 °C for 3 h. Then, aqueous solutions with appropriate amounts of Cu (copper (II) nitrate hemi (pentahydrate), Sigma Aldrich), and Fe (Iron (III)) nitrate nonahydrate, Sigma Aldrich), were added in a single step by incipient wetness impregnation and were dried overnight at 100 °C. The samples were calcined at 500 °C for 3 h. Four different formulations were prepared: 2.5%Cu/2.5%Fe, 5%Cu/2.5%Fe, 2.5%Cu/5%Fe and 5%Cu/5%Fe.

Surface area of the samples were measured according to the BET method by nitrogen adsorption at −196 °C, using a Tristar 3000 gas adsorption analyzer (Micromeritics). Structural features of the catalysts were characterized by X-ray diffraction (XRD). Philips X'Pert diffractometer was used for collecting XRD profiles (40 kV and 40 mA using Ni-filtered Cu-Kα radiation) in the range 20°–80° (step size of 0.02° and a counting time of 20 s per angular abscissa). Phase identification was carried out by the Philips X'Pert HighScore software. Redox behavior was investigated by means of temperature-programmed reduction (TPR) experiments. Samples (40 mg) were pretreated at 500 °C for 1h in air and then heated under 4.5% H₂/N₂ mixture from room temperature to 700 °C in an Autochem II 2920 Instrument (Micromeritics). H₂ consumption was monitored during the experiments.

3.2. Catalytic Activity Experiments

Aqueous solutions of ibuprofen (IBP), were prepared by dissolving 10 mg/L of ibuprofen sodium salt, C₁₃H₁₇O₂Na (Sigma-Aldrich) in ultra-pure water. A total of 100 mL of IBP solution were loaded with 200 mg/L of catalyst and 30 mL/L of H₂O₂ (3% w/w) and

heated at 70 °C for 150 min under reflux and continuous stirring conditions (500 rpm), using an Omni multistage reaction station. Hydrogen peroxide solution (3% w/w) was prepared starting from 30% w/w in H₂O from Sigma Aldrich. At the end of the reaction, samples were centrifuged in an Eppendorf Centrifuge 5804 R (5000rpm) and filtered with 0.45 µm membrane filters. The Fenton-like process was optimized, evaluating the effects of catalyst loading (200, 300 and 400 mg/L), hydrogen peroxide dose, (20, 30 and 40 mL/L), temperature (60, 70 and 80 °C) and pH (3–8, acidifying the sample with hydrochloric acid (Sigma Aldrich) or basifying the sample with sodium hydroxide (Sigma Aldrich)). The mineralization of IBP was investigated by means of the total organic carbon (TOC) (TOC-VCPN, Shimadzu analyzer (V-Series) with auto sampler). The errors in TOC measurements resulted to be within 3%. US EPA 3051 method using Inductivity Coupled Plasma—Atomic Emission Spectroscopy (ICP-AES vista pro) was used for the evaluation of the leaching of iron and copper from bimetallic catalysts during the heterogeneous Fenton process.

4. Conclusions

This study highlighted the promising activities of a series of Cu-Fe/ZrO₂ bimetallic catalysts for ibuprofen mineralization in a heterogeneous Fenton process. 5Cu/5Fe showed enhanced ibuprofen mineralization, through a relatively wider pH range, eliminating the typical constraints associated with monometallic materials. The synergistic effect of the coupled redox cycles of copper and iron boosted the catalytic activity; indeed, 5Cu/5Cu exhibited a very high and stable mineralization of ibuprofen in several cycles (75–80%) with minimal chemical (catalyst and H₂O₂ dose) and energy (i.e., temperature) inputs, resulting in a very promising material for the Fenton-like treatment of liquid waste.

Supplementary Materials: The following are available online at www.mdpi.com/article/10.3390/catal11111383/s1, Figure S1: qualitative representation of redox cycles in monometallic and bimetallic Cu-Fe catalysts, Figure S2: The extent of bimetallic and monometallic catalytic activity of the investigated catalysts.

Author Contributions: Conceptualization, E.A.; Methodology, E.A.; Investigation, S.H.; Data Curation, S.H.; Writing—Original Draft Preparation, S.H., E.A.; Writing—Review and Editing, E.A., D.G., A.T.; Funding Acquisition, A.T. All authors have read and agreed to the published version of the manuscript.

Funding: This research received no external funding.

Acknowledgments: The authors thank Acquedotto Poiana Spa for the use of the instrumentation for the TOC measurements.

Conflicts of Interest: The authors declare no conflict of interest.

References

1. O'Shea, K.E.; Dionysiou, D.D. Advanced Oxidation Processes for Water Treatment. *J. Phys. Chem. Lett.* **2012**, *3*, 2112–2113.
2. Richardson, S.D.; Ternes, T.A. Water analysis: Emerging contaminants and current issues. *Anal. Chem.* **2014**, *86*, 2813–2848.
3. Jurado, A.; Vázquez-Suné, E.; Carrera, J.; López de Alda, M.; Pujades, E.; Barceló, D. Emerging organic contaminants in ground-water in Spain: A review of sources, recent occurrence and fate in a European context. *Sci. Total Environ.* **2012**, *440*, 82–94.
4. Sun, L.; Song, H.; Li, Q.; Li, A. Fe/Cu bimetallic catalysis for reductive degradation of nitrobenzene under oxic conditions. *Chem. Eng. J.* **2016**, *283*, 366–374.
5. Lam, F.L.; Hu, X. pH-insensitive bimetallic catalyst for the abatement of dye pollutants by photo-fenton oxidation. *Ind. Eng. Chem. Res.* **2013**, *52*, 6639–6646.
6. Xu, S.; Zhu, H.; Cao, W.; Wen, Z.; Wang, J.; Francois-Xavier, C.P.; Wintgens, T. Cu-Al₂O₃-g-C₃N₄ and Cu-Al₂O₃-C-dots with dual-reaction centres for simultaneous enhancement of Fenton-like catalytic activity and selective H₂O₂ conversion to hydroxyl radicals. *Appl. Catal. B Environ.* **2018**, *234*, 223–233.
7. Duan, H.; Liu, Y.; Yin, X.; Bai, J.; Qi, J. Degradation of nitrobenzene by Fenton-like reaction in a H₂O₂/schwertmannite system. *Chem. Eng. J.* **2016**, *283*, 873–879.

8. Dükkancı, M.; Gündüz, G.; Yılmaz, S.; Prihod'Ko, R. Heterogeneous Fenton-like degradation of Rhodamine 6G in water using CuFeZSM-5 zeolite catalyst prepared by hydrothermal synthesis. *J. Hazard. Mater.* **2010**, *181*, 343–350.
9. Crane, R.A.; Scott, T.B. Nanoscale zero-valent iron: Future prospects for an emerging water treatment technology. *J. Hazard. Mater.* **2012**, *211*, 112–125.
10. Fu, F.; Dionysiou, D.D.; Liu, H. The use of zero-valent iron for groundwater remediation and wastewater treatment: A review. *J. Hazard. Mater.* **2014**, *267*, 194–205.
11. Guan, X.; Sun, Y.; Qin, H.; Li, J.; Lo, I.M.; He, D.; Dong, H. The limitations of applying zero-valent iron technology in contaminants sequestration and the corresponding countermeasures: The development in zero-valent iron technology in the last two decades (1994–2014). *Water Res.* **2015**, *75*, 224–248.
12. Sashkina, K.; Labko, V.; Rudina, N.; Parmon, V.; Parkhomchuk, E. Hierarchical zeolite FeZSM-5 as a heterogeneous Fenton-type catalyst. *J. Catal.* **2013**, *299*, 44–52.
13. Cruz, A.; Couto, L.; Esplugas, S.; Sans, C. Study of the contribution of homogeneous catalysis on heterogeneous Fe (III)/alginate mediated photo-Fenton process. *Chem. Eng. J.* **2017**, *318*, 272–280.
14. Ma, D.; Yi, H.; Lai, C.; Liu, X.; Huo, X.; An, Z.; Li, L.; Fu, Y.; Li, B.; Zhang, M.; et al. Critical review of advanced oxidation processes in organic wastewater treatment. *Chemosphere* **2021**, *275*, 130104.
15. Yamaguchi, R.; Kurosu, S.; Suzuki, M.; Kawase, Y. Hydroxyl radical generation by zero-valent iron/Cu (ZVI/Cu) bimetallic catalyst in wastewater treatment: Heterogeneous Fenton/Fenton-like reactions by Fenton reagents formed in-situ under oxic conditions. *Chem. Eng. J.* **2018**, *334*, 1537–1549.
16. Hussain, S.; Aneggi, E.; Trovarelli, A.; Goi, D. Heterogeneous Fenton-like oxidation of ibuprofen over zirconia-supported iron and copper catalysts: Effect of process variables. *J. Water Process Eng.* **2021**, *44*, 102343.
17. Vindedahl, A.M.; Strehlau, J.H.; Arnold, W.A.; Penn, R.L. Organic matter and iron oxide nanoparticles: Aggregation, interactions, and reactivity. *Environ. Sci. Nano* **2016**, *3*, 494–505.
18. Argyle, M.D.; Bartholomew, C.H. Heterogeneous Catalyst Deactivation and Regeneration: A Review. *Catalysts* **2015**, *5*, 145–269.
19. Ziylan, A.; Ince, N.H. Catalytic ozonation of ibuprofen with ultrasound and Fe-based catalysts. *Catal. Today* **2015**, *240*, 2–8.
20. Madhavan, J.; Grieser, F.; Ashokkumar, M. Combined advanced oxidation processes for the synergistic degradation of ibuprofen in aqueous environments. *J. Hazard. Mater.* **2010**, *178*, 202–208.
21. Adityosulindro, S.; Barthe, L.; González-Labrada, K.; Jáuregui Haza, U.J.; Delmas, H.; Julcour, C. Sonolysis and sono-Fenton oxidation for removal of ibuprofen in (waste)water. *Ultrason. Sonochem.* **2017**, *39*, 889–896.
22. Gagol, M.; Przyjazny, A.; Boczkaj, G. Wastewater treatment by means of advanced oxidation processes based on cavitation—A review. *Chem. Eng. J.* **2018**, *338*, 599–627.
23. Wang, X.; Zhang, X.; Zhang, Y.; Wang, Y.; Sun, S.-P.; Wu, W.D.; Wu, Z. Nanostructured semiconductor supported iron catalysts for heterogeneous photo-Fenton oxidation: A review. *J. Mater. Chem. A* **2020**, *8*, 15513–15546.
24. Clarizia, L.; Russo, D.; Di Somma, I.; Marotta, R.; Andreozzi, R. Homogeneous photo-Fenton processes at near neutral pH: A review. *Appl. Catal. B Environ.* **2017**, *209*, 358–371.
25. Adityosulindro, S.; Julcour, C.; Riboul, D.; Barthe, L. Degradation of ibuprofen by photo-based advanced oxidation processes: Exploring methods of activation and related reaction routes. *Int. J. Environ. Sci. Technol.* **2021**, 1–14.
26. Teterou, A.; Makhatova, A.; Pouloupoulos, S.G. Photochemical mineralization of Ibuprofen medicinal product by means of UV, hydrogen peroxide, titanium dioxide and iron. *Water Sci. Technol.* **2020**, *80*, 2200–2205.
27. Singh, L.; Rekha, P.; Chand, S. Cu-impregnated zeolite Y as highly active and stable heterogeneous Fenton-like catalyst for degradation of Congo red dye. *Sep. Purif. Technol.* **2016**, *170*, 321–336.
28. Hussain, S.; Aneggi, E.; Briguglio, S.; Mattiussi, M.; Gelao, V.; Cabras, I.; Zorzenon, L.; Trovarelli, A.; Goi, D. Enhanced ibuprofen removal by heterogeneous-Fenton process over Cu/ZrO₂ and Fe/ZrO₂ catalysts. *J. Environ. Chem. Eng.* **2020**, *8*, Artn103586.
29. Hussain, S.; Aneggi, E.; Goi, D. Catalytic activity of metals in heterogeneous Fenton-like oxidation of wastewater contaminants: A review. *Environ. Chem. Lett.* **2021**, *19*, 2405–2424.
30. Bokare, A.D.; Choi, W. Review of iron-free Fenton-like systems for activating H₂O₂ in advanced oxidation processes. *J. Hazard. Mater.* **2014**, *275*, 121–135.
31. Nidheesh, P.V. Heterogeneous Fenton catalysts for the abatement of organic pollutants from aqueous solution: A review. *RSC Adv.* **2015**, *5*, 40552–40577.
32. Wang, N.; Zheng, T.; Zhang, G.; Wang, P. A review on Fenton-like processes for organic wastewater treatment. *J. Environ. Chem. Eng.* **2016**, *4*, 762–787.
33. Aneggi, E.; Trovarelli, A.; Goi, D. Degradation of phenol in wastewaters via heterogeneous Fenton-like Ag/CeO₂ catalyst. *J. Environ. Chem. Eng.* **2017**, *5*, 1159–1165.
34. Adityosulindro, S.; Julcour, C.; Barthe, L. Heterogeneous Fenton oxidation using Fe-ZSM5 catalyst for removal of ibuprofen in wastewater. *J. Environ. Chem. Eng.* **2018**, *6*, 5920–5928.
35. Xia, M.; Long, M.; Yang, Y.; Chen, C.; Cai, W.; Zhou, B. A highly active bimetallic oxides catalyst supported on Al-containing MCM-41 for Fenton oxidation of phenol solution. *Appl. Catal. B Environ.* **2011**, *110*, 118–125.
36. Zhang, H.; Choi, H.J.; Huang, C.P. Optimization of Fenton process for the treatment of landfill leachate. *J. Hazard. Mater.* **2005**, *125*, 166–174. 10.1016/j.jhazmat.2005.05.025.
37. Zhou, X.; Su, T.; Jiang, Y.; Qin, Z.; Ji, H.; Guo, Z. CuO-Fe₂O₃-CeO₂/HZSM-5 bifunctional catalyst hydrogenated CO₂ for enhanced dimethyl ether synthesis. *Chem. Eng. Sci.* **2016**, *153*, 10–20.

38. Zeng, S.; Liu, K.; Chen, T.; Su, H. Influence of crystallite size and interface on the catalytic performance over the CeO₂/CuO catalysts. *Int. J. Hydrog. Energy* **2013**, *38*, 14542–14549.
39. Qu, Z.; Miao, L.; Wang, H.; Fu, Q. Highly dispersed Fe₂O₃ on carbon nanotubes for low-temperature selective catalytic reduction of NO with NH₃. *Chem. Commun.* **2015**, *51*, 956–958.
40. Zhang, L.; Nie, Y.; Hu, C.; Qu, J. Enhanced Fenton degradation of Rhodamine B over nanoscaled Cu-doped LaTiO₃ perovskite. *Appl. Catal. B Environ.* **2012**, *125*, 418–424.
41. Wang, Y.; Zhao, H.; Zhao, G. Iron-copper bimetallic nanoparticles embedded within ordered mesoporous carbon as effective and stable heterogeneous Fenton catalyst for the degradation of organic contaminants. *Appl. Catal. B Environ.* **2015**, *164*, 396–406.
42. Zhang, Y.; Zhang, K.; Dai, C.; Zhou, X.; Si, H. An enhanced Fenton reaction catalyzed by natural heterogeneous pyrite for nitrobenzene degradation in an aqueous solution. *Chem. Eng. J.* **2014**, *244*, 438–445.
43. Sabhi, S.; Kiwi, J. Degradation of 2, 4-dichlorophenol by immobilized iron catalysts. *Water Res.* **2001**, *35*, 1994–2002.
44. Lam, F.L.; Yip, A.C.; Hu, X. Copper/MCM-41 as a highly stable and pH-insensitive heterogeneous photo-Fenton-like catalytic material for the abatement of organic wastewater. *Ind. Eng. Chem. Res.* **2007**, *46*, 3328–3333.
45. Sun, Y.; Yang, Z.; Tian, P.; Sheng, Y.; Xu, J.; Han, Y.-F. Oxidative degradation of nitrobenzene by a Fenton-like reaction with Fe-Cu bimetallic catalysts. *Appl. Catal. B Environ.* **2019**, *244*, 1–10.
46. Wang, J.; Liu, C.; Li, J.; Luo, R.; Hu, X.; Sun, X.; Shen, J.; Han, W.; Wang, L. In-situ incorporation of iron-copper bimetallic particles in electrospun carbon nanofibers as an efficient Fenton catalyst. *Appl. Catal. B Environ.* **2017**, *207*, 316–325.
47. Cihanoğlu, A.; Gündüz, G.; Dükkancı, M. Degradation of acetic acid by heterogeneous Fenton-like oxidation over iron-containing ZSM-5 zeolites. *Appl. Catal. B Environ.* **2015**, *165*, 687–699.
48. Wang, Y.; Fang, J.; Crittenden, J.C.; Shen, C. Novel RGO/ α -FeOOH supported catalyst for Fenton oxidation of phenol at a wide pH range using solar-light-driven irradiation. *J. Hazard. Mater.* **2017**, *329*, 321–329.
49. Yang, X.; Tian, P.-F.; Zhang, C.; Deng, Y.-Q.; Xu, J.; Gong, J.; Han, Y.-F. Au/carbon as Fenton-like catalysts for the oxidative degradation of bisphenol A. *Appl. Catal. B Environ.* **2013**, *134*, 145–152.
50. Ramirez, J.H.; Costa, C.A.; Madeira, L.M. Experimental design to optimize the degradation of the synthetic dye Orange II using Fenton's reagent. *Catal. Today* **2005**, *107*, 68–76.
51. Guedes, A.M.; Madeira, L.M.; Boaventura, R.A.; Costa, C.A. Fenton oxidation of cork cooking wastewater—Overall kinetic analysis. *Water Res.* **2003**, *37*, 3061–3069.